Copper(II) and nickel(II) binding modes in a histidine-containing model dodecapeptide

Giuseppe Pappalardo,*[a] Giuseppe Impellizzeri,*[b] Raffaele P. Bonomo,[b] Tiziana Campagna,[a] Giulia Grasso[a] and Maria Grazia Saita[b]

[a] *Istituto di Biostrutture e Bioimmagini sezione di Catania CNR, V.Le A. Doria 6, 95125 Catania, Italy. E-mail: pappalardo@issn.ct.cnr.it*

[b] *Dipartimento di Scienze Chimiche Università di Catania, V.Le A. Doria 6, 95125 Catania Italy. E-mail: gimpellizzeri@dipchi.unict.it*

Received (in London, UK) 20th November 2001, Accepted 5th February 2002
First published as an Advance Article on the web 5th April 2002

The formation of complexes of HGGGHGHGGGHG (HG12) with copper(II) and nickel(II) have been studied in aqueous solution under various experimental conditions, including different pH and metal to ligand ratios. The study has been carried out using visible absorption, circular dichroism and electron paramagnetic resonance spectroscopic methods. Moreover, electrospray ionisation mass spectrometry has been used to directly determine the stoichiometry of the copper(II) complexes. The results indicate that HG12 can easily accommodate two metal ions in as many binding sites. The solution structure of the main complex species formed in the reaction of copper(II) with HG12 has been inferred by comparison with the copper(II) complexes formed with the shorter peptide fragments HGGGHG–NH_2 (HG6), Ac–HGGGHG–NH_2 (AcHG6) and Ac–HGGG–NH_2 (AcHG4).

With an equimolar metal to ligand ratio, the copper(II) ion binds preferentially in the N-terminal region of HG12. Conversely, Ni(II) ions form identical complexes regardless of whether the metal to ligand ratio is 1:1 or 2:1.

Finally, the circular dichroism spectra indicate a significant modification of the peptide conformation upon metal binding.

Introduction

In order to elucidate the metal-binding properties of protein domains, many studies have focused on copper(II) or nickel(II) interactions with histidine-containing peptides; the histidyl residue is known to participate in complexation with metal ions in the active sites of several metalloproteins.[1–5]

More recently, a good deal of evidence has been found in support of a close relationship between several neurodegenerative disorders, such as Alzheimer's, Parkinson's and prion diseases, and disturbances in transition metal homeostasis, especially in the central nervous system.[6] These pathologies, also named conformational diseases,[7] show altered protein conformations attributed to abnormal interactions with metal ions, which are responsible for either oxidative damage or aggregate formation. Again, histidine residues are the metal interaction sites, even if the presence of more than one histidine group does not allow the location of metal binding to be readily assessed, such as in the case of the C-terminus fragment of the prion protein.[8]

We have studied several copper(II) complexes with linear or cyclic histidine-containing peptides, and characterised them by using both thermodynamic and spectroscopic approaches.[9] From these studies, we obtained useful information on the mechanism by which these complexes exert their antioxidant activity and we addressed the relationships between the measured activity and their structural properties.[9c,e,f]

We have also used metal complexation to achieve the folding of designed oligopeptides into well-defined conformations.[10] In such an approach, the role of the metal-binding site is to serve as a device that facilitates the ordering of the peptide conformation.

In this context, it becomes important to investigate complex formation with peptide models in order to better understand the biological data. Copper(II) complexes of oligopeptides containing a single histidyl residue have been extensively studied.[1–5] It is clear from these studies that complex formation processes largely depend on several crucial factors, including the nature of the metal ion, the metal ion to ligand ratio and, especially, the location of the histidyl residue in the amino acid sequence. By contrast, less data are available on the complexation of copper ions with linear oligopeptides containing more than two histidyl residues. Histidyl side chains are expected to co-operate or compete with each other in complexing with metal ions.

In the present paper, we report the results of combined circular dichroism (CD), UV-Vis, electron paramagnetic resonance (EPR) and electrospray mass spectroscopy (ESI-MS) studies on copper(II) and nickel(II) complexes of the synthetic peptide HGGGHGHGGGHG (HG12). This study has been carried out in aqueous solution under a variety of conditions, including different pH and metal to ligand ratios. In addition, the copper(II) complexes of the shorter peptide analogues HGGGHG–NH_2 (HG6), Ac–HGGGHG–NH_2 (AcHG6) and AcHGGG–NH_2 (AcHG4) were also studied to determine, through a comparative approach, the structure of the major species formed in the reaction of copper(II) with HG12. Our data show that HG12 binds up to 2 metal ions (Cu^{2+} or

Ni^{2+}) and that upon metal binding, the peptide backbone undergoes remarkable conformational changes leading to the formation of turns or structured loops.

Experimental

Materials

All *N*-fluorenylmethoxycarbonyl (Fmoc)-protected amino-acids, 2-(1-*H*-benzotriazole-1-yl)-1,1,3,3-tetramethyluronium tetrafluoroborate (TBTU), *N*-hydroxybenzotriazole (HOBT) and Novasyn TGR resin were purchased from Novabiochem (Switzerland). PepSyn-KA resin, *N*,*N*-dimethylformamide (DMF, peptide synthesis grade) and 20% piperidine–DMF solution, were from Perseptive Biosearch. *N*,*N*-Diisopropylethylamine (DIEA), triisopropylsilane (TIS) and trifluoroacetic acid (TFA) were from Sigma/Aldrich. All other chemicals were of the highest available grade and were used without further purification.

Peptide synthesis and purification

The synthesis of AcHG4 has been reported elsewhere.[10c] The peptides HG12, HG6 and AcHG6 were synthesised on a Milligen Model 9050 peptide synthesizer using N^{α}-fluorenylmethoxycarbonyl (Fmoc) amino acids. The following amino acid derivatives Fmoc-Gly-OH and Fmoc-His(Trt)-OH were used. All residues were introduced according to the TBTU/HOBT/DIEA method.[11a] The synthesis was carried out under a two-fold excess of amino acid at every cycle and each amino acid was re-circulated through the resin for 30 min.

Each peptide was cleaved from the resin by treatment with a TFA–H_2O–TIS mixture (95:2.5:2.5 by volume) over 1.5–2.0 h. The solution containing the free peptide was filtered off from the resin, concentrated *in vacuo* at a temperature not exceeding 30 °C and then precipitated with cold freshly distilled diethyl ether. The precipitate was filtered off, desiccated under vacuum, re-dissolved in 1% AcOH–H_2O solution and then lyophilised. The peptides were purified by ion exchange chromatography by using a CM-Sephadex C-25 (NH_4^+ form) column (3 × 70 cm). The column was eluted initially with water (500 cm^3) and then with a linear gradient of aqueous NH_4HCO_3 (0–0.3 mol dm^{-3}; 2500 cm^3). Fractions were assayed by TLC and those containing the desired product (eluent: PrOH–H_2O–EtOAc–30% NH_4OH 5:3:5:1 by volume) were combined, concentrated to dryness under vacuum at 40 °C, repeatedly dissolved in water and dried to decompose any remaining ammonium hydrogencarbonate. Each pure peptide was then re-dissolved in water and lyophilised. Purity was checked further by analytical RP-HPLC (using a 150 × 4.6 mm Vydac C_{18} chromatographic column with 5 μm particle size and 300 Å pores) with a linear gradient of 0.1% TFA in water and 0.1% TFA in CH_3CN (0–5% of CH_3CN in 20 min) at a flow rate of 1 mL min^{-1}. Peptide elutions were monitored at 222 nm. The products were characterised by ^1H NMR spectroscopy and ESI-MS [HG12: m/z 1023.36 $(M+H)^+$, calcd. for $C_{40}H_{54}N_{20}O_{13}$ 1022.99; HG6: m/z 520.1 $(M+H)^+$, 542.3 $(M+Na)^+$, calcd. for $C_{20}H_{29}N_{11}O_6$ and $C_{20}H_{29}N_{11}O_6Na$ 519.2 and 542.2, respectively; AcHG6 m/z 562.1 $(M+H)^+$, 584.2 $(M+Na)^+$, calcd. for $C_{22}H_{31}N_{11}O_7$ and $C_{22}H_{31}N_{11}O_7Na$ 561.2 and 584.2, respectively].

Spectroscopic measurements

Circular dichroism (CD). The CD spectra were obtained at 25 °C under a constant flow of nitrogen on a Jasco model J-600 spectropolarimeter which had been calibrated with an aqueous solution of ammonium D-camphorsulfate.[11b] Experimental measurements were carried out in water and at different pH values using 1 mm or 1 cm path length cuvettes. The CD spectra pertinent to the free peptide ligands were recorded in the UV region (190–260 nm), whereas those in the presence of Cu^{2+} or Ni^{2+} were examined in the wavelength ranges 190–380 and 380–750 nm. The spectra represent the average of 8–20 scans. CD intensities are expressed in $\Delta\varepsilon$ (M^{-1} cm^{-1}).

Electrospray mass spectrometry (ESI-MS). Measurements were recorded on a Finnigan LCQDuo mass spectrometer using an electrospray ionisation (ESI) source fitted to a quadrupole ion trap mass analyser. ESI measurements were acquired in positive ion mode. Peptide solutions were introduced into the ESI source *via* 100 μm i.d. fused silica, from a 250 μL syringe. The experimental conditions for Cu(II)–peptide species were as follows: needle voltage 3 kV; flow rate 5 μL min^{-1}; source temperature 150 °C; m/z range 200–2000; cone potential 36 V; tube lens offset −5 V.

The complexes were prepared by dissolving the peptide HG12 and $CuSO_4$ in water at a concentration of 5×10^{-5} M and with Cu(II):HG12 ratios of 1:1, 2:1 and 5:1.

NMR spectroscopy. 4 mM solution samples were prepared in 90:10 H_2O–D_2O or pure D_2O containing trimethylsilylpropionic acid (TSP) as an internal standard. The pH of the solution was adjusted to the desired value by adding the appropriate acid or base solution. The electrode-measured pH values are uncorrected for the isotope effect. All NMR spectra were acquired at room temperature on a Varian INOVA Unity-plus spectrometer operating at 499.884 MHz. 1D spectra were generally acquired with 32 768 data points over a spectral width of 5000 Hz. 2D experiments were typically acquired with 2048 data points in the t_2 dimension and 512 t_1 increments. Water saturation was achieved by low power irradiation during the relaxation delay. ROESY spectra were run at two different mixing times, 150 and 300 ms, whereas the TOCSY experiment was acquired using a mixing time of 80 ms.

Electron paramagnetic resonance (EPR) spectroscopy. Frozen solution EPR spectra were recorded on a Bruker ER 200 D spectrometer equipped with the 3220 data system at 150 K. Copper(II) complex solutions were prepared *in situ* by mixing the necessary volume of a standard solution of $^{63}Cu(NO_3)_2$ with solutions of the peptide ligand in 1:1 or 2:1 metal to ligand ratios, and adjusting the pH of the resulting solution to the desired value by adding 10 mmol dm^{-3} KOH or HNO_3. Methanol or glycerol not exceeding 10% was added to the aqueous copper(II) complex solutions to increase resolution. Room temperature EPR spectra were obtained using a Bruker quartz aqueous solution flat cell.

Results and discussion

Metal-free ligand

The far-UV CD spectra of aqueous solutions of HG12 were recorded at different pH values (Fig. 1). The presence of a maximum at 194 nm and negative ellipticity at 208 nm in the CD curves collected in the pH range 3.0–5.0 suggests that HG12 may adopt an ordered conformation.[12]

Increasing the pH above 5.0 results in a modification of the CD pattern that shows, at pH around 7.0, a broad positive signal centred on 218 nm and negative ellipticity below 200 nm. These spectral parameters, that remain unchanged up to pH 10.0, are suggestive of the presence of an unordered peptide conformation.[12]

NMR spectra were performed at different pH values to account for the differences observed in the CD experiments. The first step was the sequence-specific assignment of the proton resonances. Table 1 lists the proton chemical shifts of

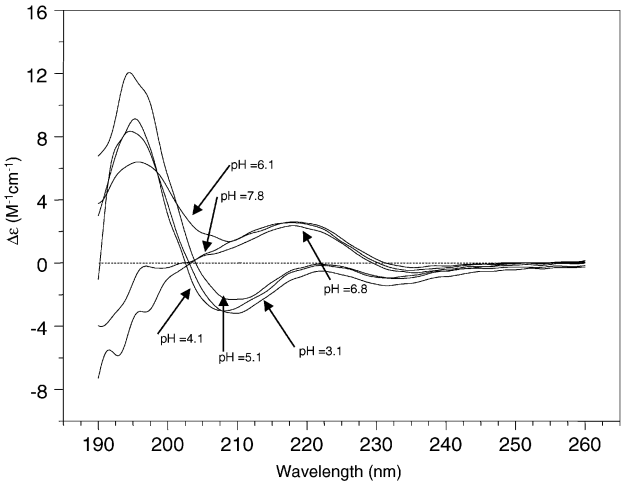

Fig. 1 CD spectra of uncomplexed HG12 ($c = 2.8 \times 10^{-4}$) in H_2O at different pH values (indicated on the curves).

HG12 in 90% H_2O–10% D_2O at pH 3. These assignments, which were complicated by the redundancy of Gly and His residues in the peptide sequence, were achieved by spin-system identification from COSY and TOCSY spectra, followed by sequential assignment through the NOE connectivities observed in the ROESY experiments.[13]

Unfortunately, the NMR experiments did not give precise information on the conformation adopted by HG12, however, the presence of appreciably intense sequential $d_{\alpha\text{-N}}$ connectivities in the ROESY spectrum carried out at acidic pH, together with the downfield shift of some CH_α proton signals, allow us to hypothesise that the peptide might adopt an extended conformation in solution.[14] Moreover, the resonances associated with the amide protons are split into two groups of signals and appear dispersed over a range of about 0.3 ppm [Fig. 2(a)]. Chemical shift dispersion of amide resonances is often an indication of a structured peptide backbone.[13]

At alkaline pH, the amide resonances were in fast exchange with the solvent and could not be observed in the NMR spectrum, thus rendering impossible any attempts at sequential assignment. Nevertheless, the spectrum acquired in D_2O at

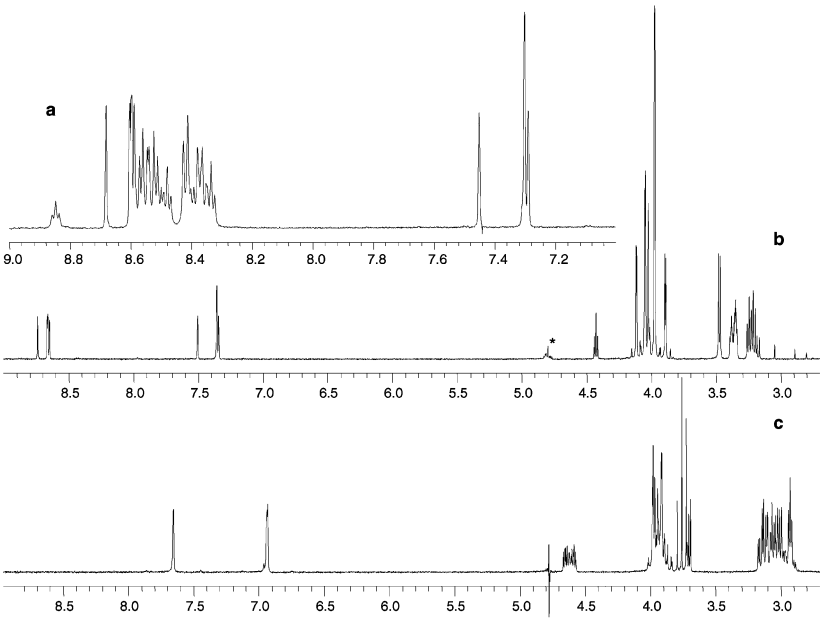

Fig. 2 500 MHz ^{1}H NMR spectra of HG12 ($c = 4.2 \times 10^{-3}$): (a) downfield region of the spectrum recorded at pH 3.0 in 90% H_2O–10% D_2O; (b) spectrum recorded in D_2O at pH 3.0 (the peak marked with an asterisk is a residual HDO signal containing residual CH_α signals from His^5, His^7 and His^{11}); (c) spectrum recorded in D_2O at pH 9.0.

Table 1 Proton chemical shifts of HG12[a]

Position	NH	α-H	β-H	Others
His^1		4.38	3.42	2H 8.68; 4H 7.45
Gly^2	8.85	4.07		
Gly^3	8.48	4.01		
Gly^4	8.35	3.93		
His$^{5\,c}$	8.53	4.74	3.30; 3.18	—[b]
Gly^6	8.51	3.93		
His$^{7\,c}$	8.52	4.79	3.32; 3.18	—[b]
Gly^8	8.57	4.01		
Gly^9	8.36	3.98		
Gly^{10}	8.33	3.93		
His$^{11\,c}$	8.41	4.79	3.30; 3.18	—[b]
Gly^{12}	8.41	3.91		

[a] Chemical shifts are expressed in δ and referenced to internal TSP. Values were measured in 9:1 H_2O–D_2O at pH 3.0 and 27 °C. [b] Sequence-specific assignment not obtained, the values are: 8.60, 8.59, 8.58 (2H); 7.30, 7.29 (4H). [c] Interchangeable values.

Table 2 Major ESI-MS peaks observed for the Cu–HG12 complexes

Species	Theoretical m/z	Experimental m/z	Species charge state	M:L stoichiometry
[CuL – 1H]	1084.3	1084.1	1+	1:1
[CuL]	542.6	542.5	2+	1:1
[CuL + 1H]	362.1	362.0	3+	1:1
[Cu_2L – 2H]	573.0	573.1	2+	2:1
[Cu_2L – 1H]	382.4	382.5	3+	2:1

pH 9.0 [Fig. 2(c)] differs from that recorded in D_2O at pH 3 [Fig. 2(b)] in that the histidine CH_α signals are shifted upfield and the imidazole signals collapse into just two singlets observable in the aromatic region. Changes are also apparent in the aliphatic region: all the signals due to both the β-CH_2 of the histidine and α-CH_2 of the glycine residues are slightly shifted upfield and appear differently dispersed. These changes can only in part be explained by the neutralisation of the positive charge on the imidazole rings and, therefore, structural changes should also be involved.

Copper(II) complexes

ESI-MS experiments were carried out to obtain information on the stoichiometry of the complex species formed by the Cu(II)–HG12 system. The values shown in Table 2 indicate that in all the spectra recorded at different pH values (pH 5.5, 7.0, 8.5) and different metal to ligand ratios (M:L 1:1; 2:1, 5:1) only 1:1 or 2:1 Cu(II)–HG12 adducts with different charge states, are observed. This indicates that HG12 can bind up to two copper(II) ions. Moreover, in the ESI-MS spectra recorded at the studied pH values, all the peaks reported in Table 2 are present. Only their relative intensities are influenced by the changing pH.

Copper(II) complexation strongly influences the solution conformation of HG12, as evidenced by the far-UV CD spectra shown in Fig. 3. In particular, the CD traces recorded with both 1:1 and 2:1 metal to ligand ratios show negative ellipticity at wavelengths >220 nm and positive dichroism in the 200–210 nm wavelength range. This spectral pattern strongly resembles that reported for peptides adopting turn conformations in solution.[12,15] The CD curves also show a pH dependence as a consequence of the different complex species which form in solution as the pH increases (Fig. 3). Finally, the dichroic bands that are present in the range 270–350 nm can be assigned to ligand to metal charge transfer transitions (LMCT).[16]

In order to determine the co-ordination modes of the Cu(II)–HG12 complex species, we resorted to a comparative study with the analogous shorter peptide fragments HG6, AcHG6 and the previously reported AcHG4[10c], and to comparison with the data reported in the literature for similar complexes.

The spectral data of the studied complexes, obtained below pH 6 in the presence of 1 molar equivalent of copper(II), are shown in Table 3. Both the Cu(II)–HG12 and Cu(II)–HG6 complexes have nearly the same λ_{max} values, whereas that of the Cu(II)–AcHG6 complex displays a red-shift. In the case of the Cu–AcHG4 system, λ_{max} at 754 nm indicates only a weak interaction with copper(II). These observations, together

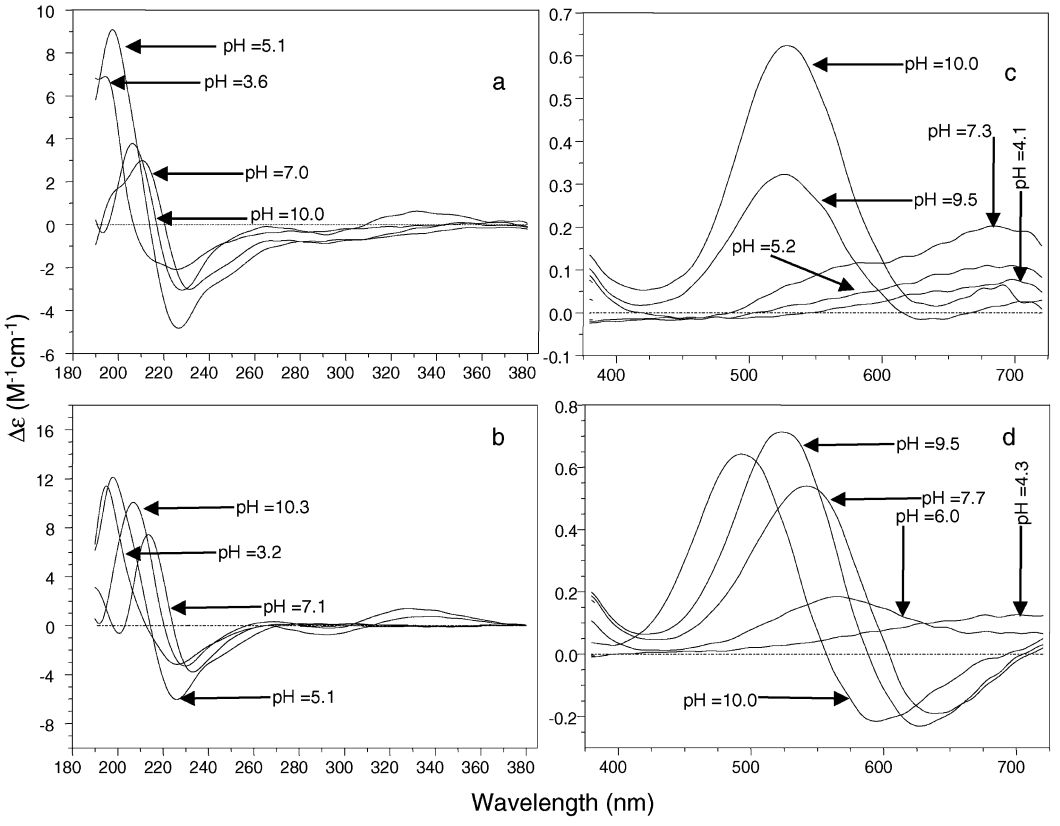

Fig. 3 CD spectra of Cu(II) complexes with HG12 measured in the UV and visible regions at various pH values (indicated on the curves) and with 1:1 (a, c) or 2:1 (b, d) M:L ratios.

Table 3 Spectroscopic data obtained at pH < 6 with a metal to ligand ratio of 1:1

Complex	pH	EPR $g_{\parallel}$; $A_{\parallel}$	UV-Vis λ_{max}/nm (ε/M^{-1} cm^{-1})	CD λ_{max}/nm ($\Delta\varepsilon$/M^{-1} cm^{-1})
Cu–HG12	5	2.275(2); 170(2)	636 (42)	680 (+0.12)[a]; 288 (−0.73)[b]
Cu–HG6	5	2.277(2); 168(2)	640 (40)	710 (+0.13)[a]
Cu–AcHG6	5	2.323(2); 136(2)	710 (22)	No signal
Cu–AcHG4[c]	5		754 (18)	No signal
Cu–Hm[d]	6	2.305; 171	681 (35)	No signal

[a] d–d Transition. [b] $NH_2 \rightarrow Cu^{2+}$ charge transfer. [c] Ref. 10(*c*). [d] Ref. 17; Hm = histamine.

with the presence of the CT band at 288 nm in the CD spectrum, suggest that the amino groups of HG12 participate in the co-ordination of the metal ion. The bidentate Cu(II)–Hm complex (Hm = histamine), in which Cu(II) is co-ordinated to the imidazole and to the amino nitrogens, displays λ_{max} at 681 nm, which is quite different from the values observed for both the Cu(II)–HG12 and Cu(II)–HG6 complexes. This indicates the formation of a 3N complex species for the Cu(II)–HG12 system. In this respect, comparison of the EPR parameters also supports this hypothesis (see Table 3).

From the above data it is possible to confirm the formation of a complex species in which the metal ion is co-ordinated to both the imidazole and amino groups of the N-terminal histidine, the third nitrogen atom presumably comes from the imidazole ring of the histidine residue in position 5 and the in-plane co-ordination is completed by an oxygen atom from a water molecule or a carbonyl group [Fig. 4(a)].

At neutral pH, both the Cu–HG12 and Cu–HG6 complexes show similar spectroscopic behaviour (very broad and weak EPR spectra and almost identical absorption maximum values; see Table 4). In contrast, the N-terminally acetylated peptide complexes behave differently, thus confirming the peculiar role of the unblocked amino group in metal complexation. The spectroscopic data, at this stage available, do not allow the structural characterisation of the complex species in solution. On the basis of the λ_{max} value for the d–d transition at 595 nm and the dichroic CT signals at 294 and 339 nm (see Table 4), we can only hypothesise that in HG12, deprotonated peptide nitrogens together with amino and imidazole nitrogens could enter into the Cu(II) co-ordination sphere.

Unprotected peptides incorporating a histidine residue at the amino terminus have been reported to readily promote the formation of dimeric copper(II) complexes.[19] The copper(II) complexes of His-Gly, His-Gly-Gly and analogous peptides also give broad EPR spectra.[20] On these bases, similar behaviour for both the Cu–HG12 and Cu–HG6 complexes at pH values near neutrality cannot be ruled out.

However, around pH 10, the EPR signals pertaining to the Cu–HG12 and Cu–HG6 systems are restored. The UV-Vis and EPR parameters listed in Table 5 for both these complexes, are consistent with 4N complex species. Moreover, the presence in their CD spectra of negative signals at 292 and 277 nm, respectively (see Table 5) suggests that the terminal amino group is still engaged in metal complexation. Interestingly, the EPR and UV-Vis parameters of the Cu–HG12 complex, are nearly identical to those reported for the Cu–

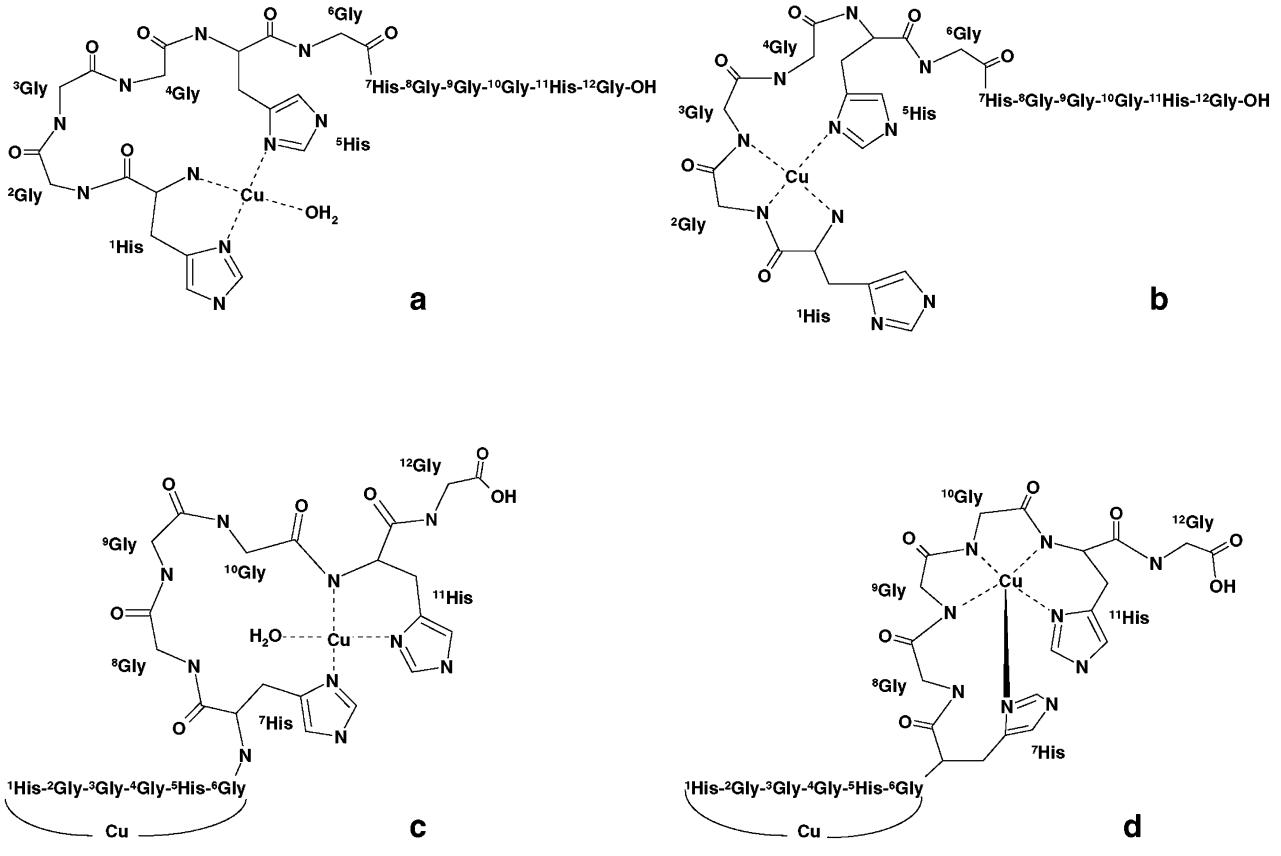

Fig. 4 Schematic representations of plausible structures for the complexes of Cu(II) with HG12: (a) pH 5 and M:L 1:1; (b) pH 10 and M:L 1:1; (c) pH 7 and M:L 2:1; (d) pH 10 and M:L 2:1. For clarity, hydrogen atoms and charges have been omitted.

Table 4 Spectroscopic data obtained at pH 7 with a metal to ligand ratio of 1:1

Complex	pH	EPR $g_{\parallel}$; $A_{\parallel}$	UV-Vis λ_{max}/nm (ε/M^{-1} cm^{-1})	CD λ_{max}/nm ($\Delta\varepsilon$/M^{-1} cm^{-1})
Cu–HG12	7	Broad spectrum	595 (90)	680 (+0.21)[a]; 575sh (+0.10)[a]; 339 (+0.27)[b]; 294 (−0.93)[c]
Cu–HG6	7	Broad spectrum	598 (61)	683 (+0.13)[a]; 584 (−0.13)[a]; 503 (+0.26)[a]
Cu–AcHG6	7	2.233(1); 182(1)	596 (70)	620 (−0.07)[a]; 512 (+0.17)[a]; 329 (+0.49)[b,d]
Cu–AcHG4[e]	7	2.231(4); 153(2)	626 (71)	720 (−0.13)[a]; 600 (+0.10)[a]; 337 (+0.21)[b]
Cu–HHGG[f]	8	Broad spectrum	569 (58)	547 (+0.41); 465 (−0.06); 337 (+0.17)
Cu–HGG[f]	8	Broad spectrum	607 (88)	700 (−0.03); 582 (+0.25)

[a] d–d Transition. [b] $N_{im} \rightarrow Cu^{2+}$ charge transfer. [c] $NH_2 \rightarrow Cu^{2+}$ charge transfer. [d] $N^- \rightarrow Cu^{2+}$ charge transfer. [e] Ref. 10(*c*). [f] Ref. 18.

Table 5 Spectroscopic data obtained at pH 10 with a metal to ligand ratio of 1:1

Complex	pH	EPR $g_{\parallel}$; $A_{\parallel}$	UV-Vis λ_{max}/nm (ε/M^{-1} cm^{-1})	CD λ_{max}/nm ($\Delta\varepsilon$/M^{-1} cm^{-1})
Cu–HG12	10.3	2.196(1); 197(2)	560 (182)	530 (+0.61)[a]; 337 (+0.62)[b]; 292 (−0.51)[c]
Cu–HG6	10.5	2.187(2); 194(2)	526 (93)	513 (+0.77)[a]; 308 (−0.11)[d]; 277 (+0.55)[c]; 250 (−0.83)[e]
Cu–AcHG6	10.5	2.205(1); 200(2)	555 (93)	601 (−0.86)[a]; 504 (+1.16)[a]; 308 (−0.64)[b]; 281 (+0.33)[d]; 254 (−1.19)[e]
Cu–AcHG4[f]	10.0	2.178(2); 194(2)	544 (86)	557 (−0.10)[a]; 332 (+0.27)[b]
Cu–GGGH[g,h]	9.0	2.194; 200	560 (125)	535 (+0.28); 308 (+0.22); 270 (−0.1); 245 (+0.24); 223 (−3.6)
Cu–GGGGH[g]	9.0	2.199; 200	560 (125)	

[a] d–d Transition. [b] $N_{im} \rightarrow Cu^{2+}$ charge transfer. [c] $NH_2 \rightarrow Cu^{2+}$ charge transfer. [d] $N^- \rightarrow Cu^{2+}$ charge transfer. [e] N_{im} $\pi_2 \rightarrow Cu^{2+}$ charge transfer. [f] Ref. 10(*c*). [g] Ref. 22. [h] Ref. 23.

Gly_3His and Cu–Gly_4His systems (see Table 5), where a NH_2, N^-, N^-, N_{im} donor set has been reported at basic pH.[21] Similarly, the pH 10 Cu–HG12 complex donor set may comprise the terminal amino group and two deprotonated peptide nitrogens from the subsequent glycine residues, with the fourth in-plane position occupied by the imidazole nitrogen from the histidine in position 5. The imidazole of the histidine residue in position 1 does not participate in metal complexation at basic pH [Fig. 4(b)].

From these data it is possible to conclude that in the presence of one molar equivalent of copper(II), the metal preferentially binds to the N-terminal binding site.

As expected, in the presence of 2 molar equivalents of copper(II), no interpretable EPR spectra were obtained (Table 6). The structure of the complex species formed with the C-terminal part of HG12 was therefore inferred by comparison with the acetylated peptides AcHG6 and AcHG4.

The EPR, absorption and CD parameters obtained for Cu–AcHG6 around pH 7 can be attributed to a 3N complex species (see Table 4). Its visible CD spectra are diagnostic of the involvement of histidyl residues with chelated adjacent ionised peptide nitrogens in metal complexation[5] [Fig. 5(a)]. Therefore, in such a complex species, the two imidazole nitrogens and the peptide nitrogen of the C-terminal histidine residue could be involved in co-ordination with copper(II).

At basic pH, the spectroscopic data shown in Table 5 for Cu–AcHG6 are consistent with the formation of a 4N complex species. The formation of this species is further confirmed by the observation of a 9-line shf pattern in the isotropic EPR spectrum (not shown). The visible CD spectrum recorded at pH 10.5 displays more intense signals, but an identical spectral shape compared to that at pH 7 [Fig. 5(a)]. On the basis of these data, we suggest that this 4N complex species might consist of three peptide nitrogens (one from the C-terminal histidine and the other two from the preceding glycines) and the imidazole nitrogen of the C-terminal histidine. On the other hand, the absorption maximum at $\lambda_{max} = 555$ nm, which is significantly red shifted as compared to similar copper(II) complexes in the literature,[20] can be explained by the axial interaction of the second imidazole side chain of the N-terminal histidine.

Interestingly, the visible CD spectra of Cu–HG12, obtained above pH 6 and in the presence of 2 molar equivalents of copper(II) show a spectral pattern which is quite similar to that seen for the Cu–AcHG6 system. This might indicate that similar co-ordination environments are provided for Cu(II) by both the C-terminal part of HG12 and the shorter analogous AcHG6 [Fig. 4(d)]. In agreement with the above, the CD spectra pertaining to the Cu–AcHG4 complex appear quite different [Fig. 5(b)], and although the spectra indicate the involvement of the histidine residue in metal co-ordination, the d–d bands occur at significantly longer wavelengths. In addition, at pH > 8.0, the spectra of the Cu–AcHG4 system undergo remarkable changes imputable to modifications of the complex's geometric features.[10c] No similar effects have been detected for either the Cu–HG12 or Cu–AcHG6 complexes. All this taken together supports the hypothesis that the Cu–AcHG6 system might reproduce the copper(II) binding modes in the C-terminal part of the dodecapeptide HG12. The structural models proposed for the complex formed at pH 7 and 10 are sketched in Fig. 4(c) and (d), respectively.

Ni(II) complexes. We also investigated the co-ordination ability of HG12 towards Ni(II) ions by using the same

Table 6 Cu(II)–HG12 spectroscopic data obtained with a 2:1 metal to ligand ratio

pH	EPR	UV-Vis λ_{max}/nm (ε/M^{-1} cm^{-1})	CD λ_{max}/nm ($\Delta\varepsilon$/M^{-1} cm^{-1})
5.0	Free copper; minor species not detectable	660 (52)	708 (+0.22)[a]
7.0	Broad spectrum	592 (154)	640 (−0.18)[a]; 540 (+0.54)[a]; 336 (+0.90)[b,c]; 290 (−0.66)[d]
10.0	Broad spectrum	571 (238)	594 (−0.21)[a]; 494 (+0.65)[a]; 330 (+1.37)[b,c]; 293 (−0.20)[d]

[a] d–d Transition. [b] $N_{im} \rightarrow Cu^{2+}$ charge transfer. [c] $N^- \rightarrow Cu^{2+}$ charge transfer. [d] $NH_2 \rightarrow Cu^{2+}$ charge transfer.

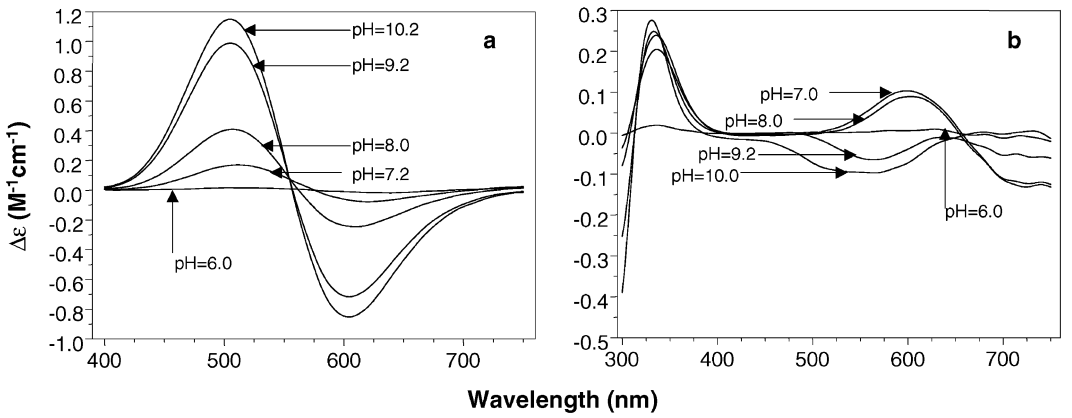

Fig. 5 Visible CD spectra at various pH values (indicated on the curves) for Cu(II)–AcHG6 (a) and Cu(II)–AcHG4 (b) complexes.

approach described above for the copper(II) complexes. The far-UV CD experiments indicate that only above pH 8 do the Ni(II)–HG12 complexes exhibit CD spectra with maxima and minima in the wavelength ranges expected for turn conformations,[12,15] resembling those collected in the presence of Cu(II) (Fig. 6). Interestingly, at these pH values, both the visible absorption and CD spectra indicate the formation of square planar complexes. The formation of such diamagnetic species suggests the engagement of four nitrogen atoms in metal co-ordination.[18] By contrast, our data indicate that between pH 5 and *ca.* 8 the complexed Ni(II) ions are mainly in an octahedrical environment.[22]

Furthermore, in the presence of Ni(II), the visible CD spectra strongly indicate the engagement of histidyl residues with chelated adjacent ionised peptide nitrogens in metal ion co-ordination for both 1:1 and 2:1 metal to ligand ratios (Fig. 6).[5] This fact argues for the strict similarity of the two metal-binding sites. Moreover, both the visible absorption and CD spectra show remarkable analogies with those reported for the Ni–GGH and Ni–AcGGGH complexes.[24] In these systems, the abstraction of the three adjacent peptide-bond hydrogens, together with the imidazole nitrogen, results in a 4N co-ordinated complex in slightly alkaline solution.[24] Therefore, it was thought that comparison with the square planar Ni(II)–AcHG4 complex would definitely clarify the binding mode of the Ni(II) ions to HG12. Both the UV-Vis and CD spectra obtained at pH 10 suggest the formation of a square planar Ni^{2+} complex species. Interestingly, the dichroic signals of the d–d transition are not only weaker than those observed in the Ni(II)–HG12 system, but they also display an opposite order in that the long wavelength band is positive and the short one negative (Fig. 7). All these facts taken together allow the conclusion that both Ni(II) ions, in the respective binding sites, co-ordinate in a square planar environment consisting of three consecutive deprotonated peptide nitrogens and one imidazole nitrogen. Neither the N-terminal histidine residue

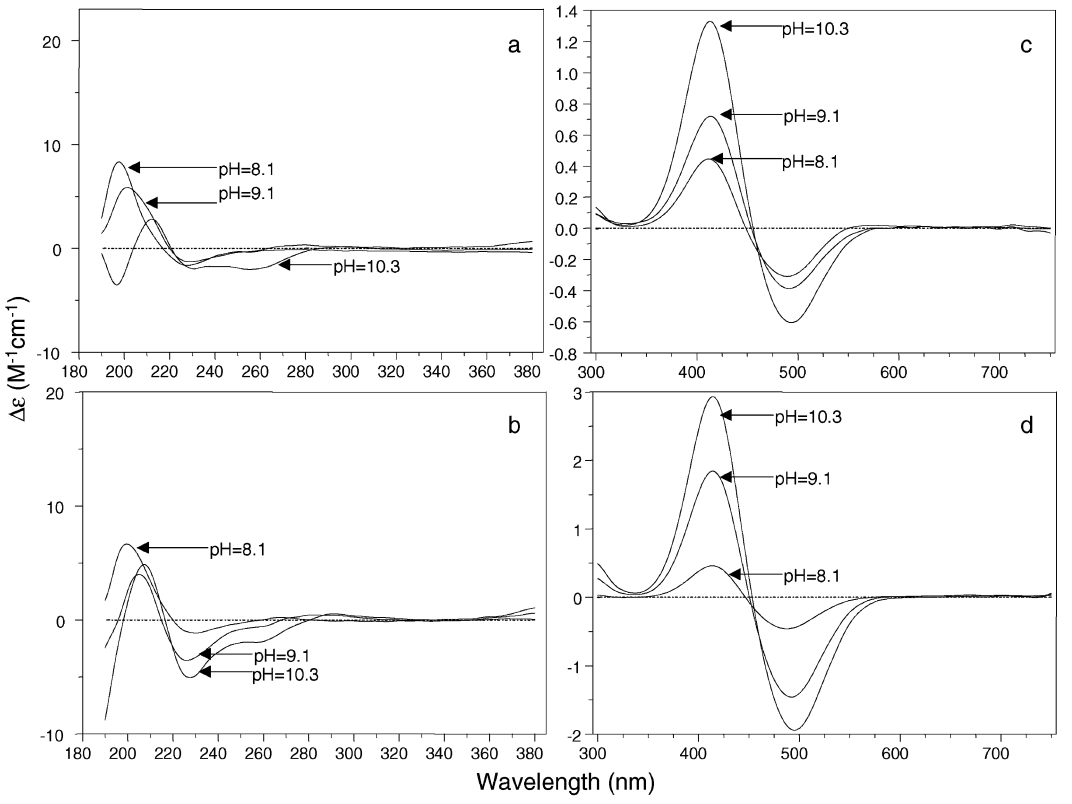

Fig. 6 CD spectra of Ni(II) complexes with HG12 measured in the UV and visible regions at various pH values (indicated on the curves) and with 1:1 (a, c) or 2:1 (b, d) M:L ratios.

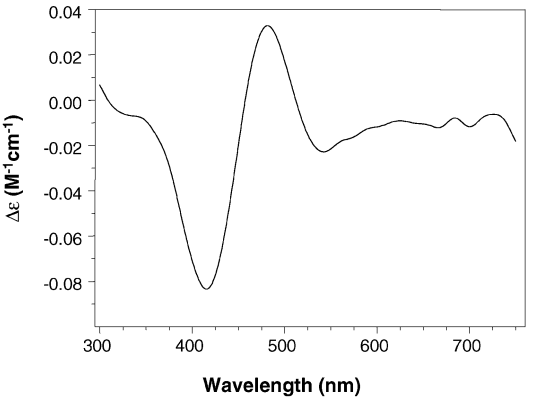

Fig. 7 Visible CD spectrum of the Ni(II)–AcHG4 complex at pH 10.

nor the histidine in position 7 participate in metal complexation.

Concluding remarks

This work demonstrates that the studied peptide, HG12, is capable of co-ordinating two copper(II) or Ni(II) ions. CD studies reveal that peptide conformation is remarkably affected by copper(II) complexation, even at low pH. The recorded spectra suggest the formation of turns or structured loops upon metal binding. On the other hand, Ni(II) ions behave differently because only at basic pH do they effectively induce a conformational transition similar to that observed for copper(II). Interestingly, at these high pH values, Ni(II) forms planar diamagnetic 4N complex species consisting of imidazole and deprotonated peptide nitrogens. The analysis of the CD and NMR data seems to indicate that both the metal anchoring the imidazole side chains at low pH and the deprotonation at the peptide histidyl nitrogens at higher pH are important determinants for the observed *ordering* of the polypeptide chain. The structural model proposed in this work may provide the starting point for evaluating the metal ion-inducing secondary structure in designed peptides, as well as in protein systems.

Acknowledgements

We acknowledge CNR Agenzia 2000 project CNRC00781B and MURST PRIN 2000 project MM03194891 for financial support. We also thank Prof. Enrico Rizzarelli for helpful discussions.

References

1 H. Kozlowsky, W. Bal, M. Dyba and T. Kowlik-Jankowska, *Coord. Chem. Rev.*, 1999, **184**, 319.
2 L. D. Pettit and R. A. Robbins, "Metal-Peptide Complex Formation" in *Handbook of Metal Ligand Interaction in Biological Fluids*, ed. G. Berthon, Marcel Dekker, New York, 1995, vol. 1, p. 636.
3 I. Sovago, "Metal Complexes of Peptides and Their Derivatives" in *Biocoordination Chemistry*, ed. K. Burger, Ellis Horwood, Chichester, 1990, ch. IV. p. 135.
4 H. Sigel and R. B. Martin, *Chem. Rev.*, 1982, **82**, 385.
5 R. J. Sundberg and R. B. Martin, *Chem. Rev.*, 1974, **74**, 471.
6 (*a*) A. I. Bush, *Curr. Opin. Chem. Biol.*, 2000, **4**, 184; (*b*) D. J. Waggonner, T. B. Bartnikas and J. D. Gitlin, *Neurobiol. Dis.*, 1999, **6**, 221; (*c*) L. M. Sayre, G. Perry and M. A. Smith, *Curr. Opin. Chem. Biol.*, 1999, **3**, 220.
7 M. Pocchiari, *Mol. Aspects Med.*, 1994, **15**, 195.
8 G. M. Cereghetti, A. Schweiger, R. Glockshuber and S. Van Doorslaer, *Biophys. J*, 2001, **81**, 516.
9 (*a*) G. Arena, R. P. Bonomo, R. M. Izatt, J. D. Lamb and E. Rizzarelli, *Inorg. Chem.*, 1987, **26**, 795; (*b*) G. Arena, R. P. Bonomo, L. Casella, M. Gullotti, G. Impellizzeri, G. Maccarrone and E. Rizzarelli, *J. Chem. Soc., Dalton Trans.*, 1991, 3203; (*c*) R. P. Bonomo, F. Bonsignore, E. Conte, G. Impellizzeri, G. Pappalardo, R. Purrello and E. Rizzarelli, *J. Chem. Soc., Dalton Trans.*, 1993, 1295; (*d*) G. Arena, G. Impellizzeri, G. Maccarrone, G. Pappalardo and E. Rizzarelli, *J. Chem. Soc., Dalton Trans.*, 1994, 1227; (*e*) R. P. Bonomo, E. Conte, G. Impellizzeri, G. Pappalardo, R. Purrello and E. Rizzarelli, *J. Chem. Soc., Dalton Trans.*, 1996, 3093; (*f*) R. P. Bonomo, G. Impellizzeri, G. Pappalardo, R. Purrello, E. Rizzarelli and G. Tabbì, *J. Chem. Soc., Dalton Trans.*, 1998, 3851.
10 (*a*) R. P. Bonomo, L. Casella, L. De Gioia, G. Impellizzeri, H. Molinari, T. Jordan, G. Pappalardo, R. Purrello and E. Rizzarelli, *J. Chem. Soc., Dalton Trans.*, 1997, 2387; (*b*) G. Impellizzeri, G. Pappalardo, R. Purrello, E. Rizzarelli and A. M. Santoro, *Chem. Eur. J.*, 1998, **4**, 1791; (*c*) R. P. Bonomo, G. Impellizzeri, G. Pappalardo, E. Rizzarelli and G. Tabbì, *Chem. Eur. J.*, 2000, **6**, 4195.
11 (*a*) R. Knorr, A. Trzeciek, W. Bannworth and D. Gillessen, *Tetrahedron Lett.*, 1989, **30**, 1927; (*b*) G. C. Chen and J. T. Yang, *Anal. Lett.*, 1977, **10**, 1195.
12 A. Perczel and M. Hòllosi, in *Circular Dichroism and the Conformational Analysis of Biomolecules*, ed. G. D. Fasman, Plenum, New York, 1996, p. 295.
13 K. Wüthrich, *NMR of Proteins and Nucleic Acids*, Wiley, New York, 1986.
14 K. Wüthrich, M. Billeter and W. Brown, *J. Mol. Biol.*, 1984, **180**, 715.
15 (*a*) R. W. Woody, in *Peptides, Polypeptides and Proteins*, ed. E. R. Blout, F. A. Bovey, M. Goodman and L. Lotan, Wiley, New York, 1974, p. 338; (*b*) M. C. Manning, M. Illangasekare and R. Woody, *Biophys. Chem.*, 1988, **31**, 77.
16 (*a*) J. M. Tsangaris, J. W. Chang and R. B. Martin, *J. Am. Chem. Soc.*, 1969, **91**, 726; (*b*) T. G. Fawcett, E. E. Bernarducci, K. Krough-Jespersen and H. J. Schugar, *J. Am. Chem. Soc.*, 1980, **102**, 2598.
17 R. P. Bonomo, V. Cucinotta, F. D'Allessandro, G. Impellizzeri, G. Maccarrone, G. Vecchio and E. Rizzarelli, *Inorg. Chem.*, 1991, **30**, 2708.
18 L. D. Pettit, J. E. Gregor and H. Kozlowsky, in *Perspectives on Bioinorganic Chemistry*, ed. R. W. Hay, J. R. Dilworth and K. B. Nolan, Jai Press, London, 1991, vol. 1, p. 1.
19 H. Aiba, A. Yokoyama and H. Tanaka, *Bull. Chem. Soc. Japan*, 1974, **47**, 136.
20 J. Ueda, N. Ikota, A. Hanaki and K. Koga, *Inorg. Chim. Acta*, 1987, **135**, 43.
21 K. Varnagy, J. Szabò, I. Sovago, G. Malandrinos, N. Hadjiliados, D. Sanna and G. Micera, *J. Chem. Soc., Dalton Trans.*, 2000, 467.
22 R. B. Martin, in *Metal Ions in Biological Systems*, ed. H. Sigel and A. Sigel, Marcel Dekker, New York, 1988, vol. 1, p. 123.
23 L. D. Pettit, S. Pyburn, W. Bal, H. Kozlowski and M. Bataille, *J. Chem. Soc., Dalton Trans.*, 1990, 3565.
24 (*a*) G. F. Bryce, R. W. Roeske and F. R. N. Gurd, *J. Biol. Chem.*, 1965, **240**, 3837; (*b*) G. F. Bryce, R. W. Roeske and F. R. N. Gurd, *J. Biol. Chem.*, 1966, **241**, 1072.